

Photovoltaic Cell Parameter Estimation Using Moth-Flame Optimization Algorithm

Fitriah Husin^{1*}, Ayong Hiendro²

¹ Department of Electrical Engineering, Tanjungpura University, Pontianak, Indonesia.

² Department of Mechanical Engineering, Tanjungpura University, Pontianak, Indonesia.

Received: March 15, 2025

Revised: May 09, 2025

Accepted: July 25, 2025

Published: July 31, 2025

Corresponding Author:

Fitriah Husin

fitriah@ee.untan.ac.id

DOI: [10.29303/jppipa.v11i7.10892](https://doi.org/10.29303/jppipa.v11i7.10892)

© 2025 The Authors. This open access article is distributed under a (CC-BY License)



Abstract: Estimation of photovoltaic cell parameters from experimental data is an important part of photovoltaic system performance modeling and optimization. This study aims to estimate the parameters of photovoltaic cells. The photovoltaic models used are the one-diode model (ODM) and the two-diode model (TDM). Optimization is performed using the moth-flame optimization (MFO) algorithm. The root mean square error (RMSE) method is applied to determine the accuracy of the estimated parameters. Experimental results show that the MFO algorithm is able to obtain photovoltaic cell parameters with a high level of accuracy, both in ODM and TDM. The current-voltage (I-V) and power-voltage (P-V) curves between the measured and estimated data also show a very good match. In addition, the optimization algorithm outperforms most metaheuristic algorithms applied in photovoltaic cell parameter determination. Thus, the MFO algorithm is suitable to be applied in determining the photovoltaic cell parameters.

Keywords: Metaheuristic algorithm; One-diode model; Photovoltaic parameters; Two-diode model.

Introduction

Solar energy has emerged as a cornerstone of global efforts to transition toward sustainable energy systems due to its abundance, renewability, and low environmental impact (Jannah et al., 2024). The design of solar power plants typically begins with computational analysis and simulation, where precise photovoltaic (PV) cell modeling serves as a critical initial step to optimize plant performance. This process relies on mathematical models to derive PV parameters, enabling the generation of current-voltage (I-V) and power-voltage (P-V) characteristics that align with the operational behavior of the cells. However, PV cell modeling is inherently complex due to its nonlinear nature and significant sensitivity to environmental variables, including temperature fluctuations and variations in solar irradiance (Bălăceanu et al., 2024; Nfaoui et al., 2024). These factors necessitate robust modeling frameworks to ensure accuracy across diverse

operating conditions. These sensitivities necessitate the development of robust and flexible modeling frameworks that maintain accuracy across diverse environmental conditions.

Mathematical models for I-V and P-V characterization involve numerous unknown variables, yet the one-diode and two-diode models are widely adopted for their ability to generate accurate results (Tifidat et al., 2022). The one-diode model, requiring only five parameters, offers simplicity and computational efficiency. However, its accuracy diminishes under low irradiance conditions due to the neglect of recombination losses (Lin et al., 2024). In contrast, the two-diode model incorporates seven parameters, addressing this limitation by reintroducing recombination effects through an additional diode. This enhancement improves reliability in scenarios with variable solar radiation, positioning the two-diode model as a superior choice for high-precision PV system design and optimization.

How to Cite:

Husin, F., & Hiendro, A. (2025). Photovoltaic Cell Parameter Estimation Using Moth-Flame Optimization Algorithm. *Jurnal Penelitian Pendidikan IPA*, 11(7), 779–788. <https://doi.org/10.29303/jppipa.v11i7.10892>

Regardless of the model selected, the accuracy of PV modeling heavily depends on the proper estimation of its parameters, which define the shape and accuracy of the I-V and P-V curves. These parameters are not directly measurable and must be inferred through optimization techniques. However, due to the highly nonlinear and multimodal nature of the objective function, identifying optimal parameters presents a complex and computationally intensive challenge. This makes parameter estimation a critical focus in PV research, as even slight inaccuracies can lead to substantial deviations in performance predictions.

The determination of parameters in the one-diode and two-diode models constitutes an optimization challenge requiring advanced computational solutions. Three primary approaches are employed to address this issue: analytical methods, numerical methods, and metaheuristic algorithms. Analytical techniques, such as the Padé approximation (Wang et al., 2024), Taylor series expansion (El Ainaoui et al., 2023), and Lambert W function (Abdel-Basset et al., 2024; Pindado et al., 2021), offer rapid computational efficiency and reasonable accuracy for parameter extraction. However, their applicability diminishes for complex or large-scale problems due to inherent limitations in handling nonlinearities and excessive computational demands.

Numerical methods, including Newton-Raphson (Abdulrazzaq et al., 2022; Adak et al., 2023) and Gauss-Seidel (Sakthivel et al., 2023) iterations, enhance accuracy by leveraging comprehensive curve data points. While these methods outperform analytical approaches in precision, they are hindered by high computational resource requirements, susceptibility to non-convergence, and a tendency to stagnate at local optima (Tifidat et al., 2023). In contrast, metaheuristic algorithms have gained prominence for their robustness in resolving intricate optimization problems. These algorithms eliminate dependencies on strict convexity, continuity, or differentiability of objective functions and constraints, enabling superior performance in accuracy, reliability, and convergence speed compared to traditional methods (Bakir, 2023). By deploying randomized search agents across the solution space, metaheuristic strategies effectively circumvent local optima, ensuring global optimization potential (Kwakye et al., 2024). This adaptability makes them particularly advantageous for photovoltaic parameter identification in scenarios demanding high precision and computational stability.

Numerous metaheuristic algorithms have been developed and utilized for photovoltaic parameter estimation to derive current-voltage (I-V) characteristics. A notable example is the genetic algorithm (GA) (Durango-Flórez et al., 2022; Saadaoui et al., 2021), which

mitigates the risk of convergence at local optima by performing search operations across multiple points simultaneously. Despite its ability to explore diverse solutions, GA exhibits a slow convergence rate, limiting its efficiency. Alternative approaches, such as the differential evolution (DE) algorithm (Yuan et al., 2023), particle swarm optimization (PSO) algorithm (Lo et al., 2024), and simulated annealing (SA) algorithm (Dkhichi, 2023), have been employed to enhance the precision of parameter estimation. Comparative studies indicate that DE, PSO, and SA demonstrate superior accuracy over GA in identifying photovoltaic parameters.

While DE is recognized for its robustness in solving optimization problems, its effectiveness heavily depends on appropriate parameter configurations [18]. In contrast, PSO offers rapid convergence but is prone to stagnation in local optima, particularly in high-dimensional search spaces (Lo et al., 2024). SA, renowned for its adaptability and global optimization capabilities, often demands extensive computational resources and time to achieve optimal solutions (Dkhichi, 2023). These trade-offs highlight the need for algorithm selection based on specific requirements, balancing accuracy, computational efficiency, and problem dimensionality in photovoltaic parameter estimation.

This study introduces a metaheuristic moth-flame optimization (MFO) algorithm designed to enhance the accuracy and efficiency of photovoltaic parameter estimation in both single-diode and double-diode models. The proposed MFO algorithm demonstrates superior performance compared to conventional optimization methods, addressing critical challenges in parameter extraction while precisely generating current-voltage (I-V) and power-voltage (P-V) characteristics of photovoltaic cells. By leveraging the algorithm's robust search mechanisms, this approach achieves higher precision in modeling photovoltaic behavior, offering a reliable solution for optimizing energy output predictions in solar energy systems.

Method

Photovoltaic cell behavior is commonly modeled through equivalent circuit representations, which integrate key electrical components such as a photogenerated current source, diode configurations (in series or parallel), series resistance, and shunt resistance. Among the established modeling frameworks, two predominant configurations are widely adopted: one-diode model (ODM) and two-diode model (TDM).

The ODM simplifies the photovoltaic cell's electrical characteristics using a single diode to simulate recombination losses in the depletion region. In contrast,

the TDM incorporates an additional diode to account for recombination effects in both the neutral and depletion regions, enhancing modeling accuracy under varying operating conditions. These models serve as foundational tools for simulating current-voltage (I-V) and power-voltage (P-V) curves, enabling precise parameter extraction critical for optimizing photovoltaic system performance.

One-Diode Model (ODM)

The equivalent circuit of the ODM for photovoltaic cells is depicted in Figure 1. This model comprises four primary components: a photogenerated current source (I_{PV}), a diode, a series resistance (R_S), and a shunt resistance (R_P). The current source represents the photogenerated current, which arises from the conversion of incident solar energy into electrical energy through electron-hole pair generation. The diode accounts for carrier recombination dynamics, with the diode current (I_D) corresponding to the diffusion current produced by majority carriers under forward bias (Morcillo et al., 2022).

The series resistance quantifies the internal resistive losses within the semiconductor material and metallic contacts, leading to voltage and power dissipation as current flows through the cell. Conversely, the shunt resistance models leakage currents across the p-n junction, which degrade the cell's efficiency under non-ideal conditions. The diffusion current is governed by the diode equation:

$$I_D = I_0 \left\{ \exp \left[\frac{(V+IR_S)}{AV_{TH}} \right] - 1 \right\} \quad (1)$$

Based on the equivalent circuit in Figure 1, the output current of the photovoltaic cell by the ODM can be expressed as follows:

$$I = I_{PV} - I_D - \frac{V+IR_S}{R_P} \quad (2)$$

In equations (1) and (2), I_{PV} is the photogeneration current, I_0 is the reverse saturation current, A is the ideality factor of the diode, V is the photovoltaic output voltage, I is the photovoltaic output current, and V_{TH} is the thermal voltage. Thermal voltage is defined as follows:

$$V_{TH} = \frac{N_S k T}{q} \quad (3)$$

The thermal stress V_{TH} depends on N_S (number of photovoltaic cells connected in series), k (Boltzmann constant = 1.38×10^{-23} J/K), q (electron charge = 1.6×10^{-19} C), and T (absolute temperature of the photovoltaic cell measured in Kelvin). Thus, in the ODM there are five

parameters namely: I_{PV} , I_0 , R_S , R_P , and A , as unknown parameters.

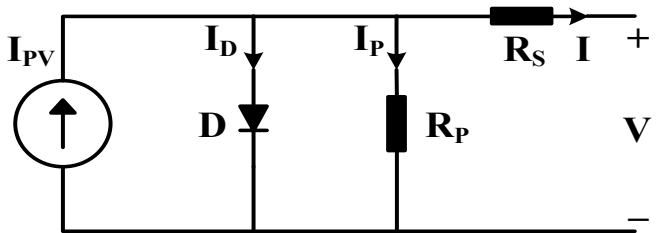


Figure 1. One-diode model circuit

Two-Diode Model (TDM)

The equivalent circuit of the TDM for photovoltaic cells, illustrated in Figure 2, incorporates two diodes to enhance the representation of carrier dynamics, contrasting with the simplified TDM. This configuration explicitly accounts for recombination losses in both the depletion and neutral regions of the p-n junction, addressing limitations of the TDM in capturing non-ideal behaviors under diverse operating conditions (Çelik et al., 2025). The first diode models the diffusion current (I_{D1}) arising from majority carrier transport, while the second diode represents the recombination current (I_{D2}) associated with minority carrier dynamics, enabling a more comprehensive characterization of photovoltaic cell performance. The diffusion current and recombination current are governed by distinct diode equations:

$$I_{D1} = I_{01} \left\{ \exp \left[\frac{(V+IR_S)}{A_1 V_{TH}} \right] - 1 \right\} \quad (4)$$

$$I_{D2} = I_{02} \left\{ \exp \left[\frac{(V+IR_S)}{A_2 V_{TH}} \right] - 1 \right\} \quad (5)$$

In equations (4) and (5), I_{01} and I_{02} are the reverse saturation currents due to diffusion and recombination phenomena, respectively. The ideality factors of diffusion and recombination are denoted by A_1 and A_2 , respectively. Thus, the output current is as follows:

$$I = I_{PV} - I_{D1} - I_{D2} - \frac{V+IR_S}{R_P} \quad (6)$$

For the TDM there are seven unknown parameters, namely: I_{PV} , I_0 , R_S , R_P , A_1 and A_2 .

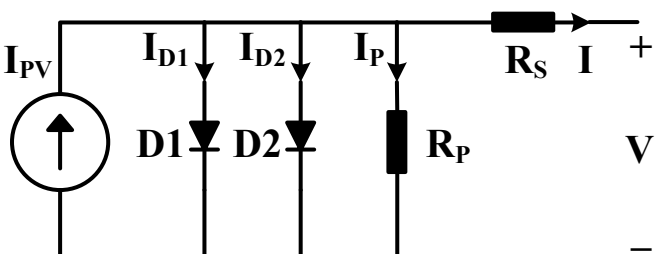


Figure 2. Two-diode model circuit

Problem Formulation

The optimization framework in this study is formulated as an optimization problem defined by a specific objective function. To quantify the accuracy of parameter estimation, the root mean square error (RMSE) method (Calasan et al., 2024) is employed as the objective function. RMSE serves as a statistical metric to evaluate the deviation between experimentally measured current-voltage (I-V) data and the corresponding values estimated by the photovoltaic model. This approach ensures rigorous minimization of discrepancies, enabling precise calibration of model parameters to match empirical observations.

The objective function for the photovoltaic parameter estimation problem is mathematically expressed as:

$$RMSE = \sqrt{\frac{1}{N} \sum_{k=1}^N [f_k(V, I, \emptyset)]^2} \quad (7)$$

In equation (7), N is the number of measurement data, V and I are the photovoltaic output voltage and current (measurement results) and \emptyset is a vector containing the parameters to be calculated. For the ODM the function $f_k(V, I, \emptyset)$ is:

$$f_k(V, I, \emptyset) = I_{PV} - I_D - \frac{V + IR_S}{R_p} - I \quad (8)$$

While for MDD the function $f_k(V, I, \emptyset)$ is:

$$f_k(V, I, \emptyset) = I_{PV} - I_{D1} - I_{D2} - \frac{V + IR_S}{R_p} - I \quad (9)$$

The vector \emptyset for the ODM contains $\emptyset = \{I_{PV}, I_o, R_s, R_p, A\}$ and for the TDM contains $\emptyset = \{I_{PV}, I_o, R_s, R_p, A_1, A_2\}$.

Moth-Flame Optimization Algorithm

The moth-flame optimization (MFO) algorithm operates within a structured metaheuristic framework, comprising six sequential phases: parameter initialization, population generation, fitness evaluation, iterative updating, position refinement, and solution selection [24]. In this methodology, moths act as search agents navigating a multidimensional solution space, while flames represent the optimal positions identified during the exploration process. Each moth dynamically adjusts its position relative to the nearest flame, iteratively refining its trajectory to converge toward regions of higher fitness, thereby balancing global exploration and local exploitation.

Critical algorithmic parameters include the population size (N), dimensionality of the problem,

lower (lb) and upper bounds (ub) of the search space, and the maximum iteration count (Max). The bounds lb and (ub) constrain the solution domain, ensuring feasible parameter ranges for photovoltaic models. These boundaries are mathematically defined as:

$$lb_j = [lb_1 \ lb_2 \ \dots \ lb_D] \quad (10)$$

$$ub_j = [ub_1 \ ub_2 \ \dots \ ub_D] \quad (11)$$

In the MFO algorithm, the moth population is randomly generated using equations:

$$M_{i,j}^{(I=1)} = lb_j + rand_j \cdot (ub_j - lb_j) \quad (12)$$

Furthermore, the moth population can be presented in matrix form as follows:

$$M_{i,j}^{(I)} = \begin{bmatrix} M_{1,1} & M_{1,2} & \dots & M_{1,D} \\ M_{2,1} & M_{2,2} & \dots & M_{2,D} \\ M_{3,1} & M_{3,2} & \dots & M_{3,D} \\ \vdots & \vdots & \ddots & \vdots \\ M_{N,1} & M_{N,2} & \dots & M_{N,D} \end{bmatrix} \quad (13)$$

In equations (12) and (13), the values of $i = 1, 2, 3, \dots, N$ and $j = 1, 2, 3, \dots, D$.

The process to find the fitness value of the moth is done using the equation:

$$MF_i^{(I=1)} = f(M_{i,j}^{(I=1)}) \quad (14)$$

Furthermore, the fitness value can be presented in matrix form as follows:

$$MF_i^{(I)} = \begin{bmatrix} MF_1 \\ MF_2 \\ MF_3 \\ \vdots \\ MF_N \end{bmatrix} \quad (15)$$

In equations (14) and (15), the values of $i = 1, 2, 3, \dots, N$ and $j = 1, 2, 3, \dots, D$.

The flame fitness values (at $I = 1$) are the initial fitness values of the sorted moths, while the flames are then sorted based on their match values. The flame fitness values are sorted from best to worst, as follows:

$$FF_i^{(I)} = sorted(MF_i^{(I)}) = \begin{bmatrix} FF_1 \\ FF_2 \\ FF_3 \\ \vdots \\ FF_N \end{bmatrix}^{(I)} \quad (16)$$

$$F_{i,j}^{(I)} = \begin{bmatrix} F_{1,1} & F_{1,2} & \dots & F_{1,D} \\ F_{2,1} & F_{2,2} & \dots & F_{2,D} \\ F_{3,1} & F_{3,2} & \dots & F_{3,D} \\ \vdots & \vdots & \ddots & \vdots \\ F_{N,1} & F_{N,2} & \dots & F_{N,D} \end{bmatrix}^{(I)} \quad (17)$$

Updating the moth population is using a logarithmic spiral model, in which the movement of moths will converge to the flame based on the formulation:

$$M_{i,j}^{(I+1)} = S_{i,j}^{(I)} \cdot e^{(bt)} \cdot \cos(2\pi t) + F_{i,j}^{(I)} \quad (18)$$

where S is the distance between the moth and the flame, b is the shape constant of the spiral path ($-1 \leq b \leq 1$), t is the control parameter to keep and adjust the distance between the moth and the flame to always be in the spiral path ($r \leq t \leq 1$), and r is the convergence constant that moves down from -1 to -2 to make the forecast value of the control parameter.

Furthermore, the distance between the moth and the flame is defined as follows:

$$S_{i,j}^{(I)} = \text{abs}(F_{i,j}^{(I)} - M_{i,j}^{(I)}) \quad (19)$$

The r and t values are respectively expressed as follows:

$$r = -\left(1 + \frac{I}{Max}\right) \quad (20)$$

$$t = \text{rand.}(r - 1) + 1 \quad (20)$$

The updated position of the moth may sometimes become worse after going through the iteration process. To ensure that the moth can find the flame, the moth must always update its position with respect to the flame at each final step of the iteration process. Therefore, the control parameters required for this mechanism are:

$$FN = \text{round}\left(N - \frac{(N-1)I}{Max}\right) \quad (21)$$

Finally, based on (22), the process of moth population renewal becomes:

$$M_{i,j}^{(I+1)} = S_{i,j}^{(I)} \cdot e^{(bt)} \cdot \cos(2\pi t) + F_{i,j}^{(I)}, \text{ if } I \leq FN \quad (23)$$

$$M_{i,j}^{(I+1)} = S_{i,j}^{(I)} \cdot e^{(bt)} \cdot \cos(2\pi t) + F_{FN,j}^{(I)}, \text{ if } I > FN \quad (24)$$

Next, the flame update is done using the equation:

$$FF_i^{(I+1)} = \text{sorted} \begin{bmatrix} MF_i^{(I+1)} \\ FF_i^{(I)} \end{bmatrix} \quad (25)$$

The position of the flames in order of their fitness value becomes:

$$F_{i,j}^{(I+1)} = \begin{bmatrix} F_{1,1} & F_{1,2} & \dots & F_{1,D} \\ F_{2,1} & F_{2,2} & \dots & F_{2,D} \\ F_{3,1} & F_{3,2} & \dots & F_{3,D} \\ \vdots & \vdots & \ddots & \vdots \\ F_{N,1} & F_{N,2} & \dots & F_{N,D} \end{bmatrix}^{(I+1)} \quad (26)$$

The best position of the moth and its fitness value are selected here, as follows:

$$FF_{best}^{(I+1)} = FF_1^{(I+1)} \quad (27)$$

$$F_{best}^{(I+1)} = F_{1,j}^{(I+1)} \quad (28)$$

The process of updating moths and flames can then be carried out again until $FF_{best}^{(I+1)}$ reaches the predetermined criterion value and/or $I = Max$.

Result and Discussion

The experimental current-voltage (I-V) characteristics of the RTC-France photovoltaic cell, measured under standard test conditions (33°C , 1000 W/m^2 irradiance), are summarized in Table 1. For parameter estimation, the one-diode model (ODM) involves five unknown variables: the photogenerated current, diode reverse saturation current, ideality factor, series resistance), and shunt resistance. MFO algorithm is applied to estimate these parameters within the following constrained search intervals: $I_{PV} = \{0, 1\} \text{ A}$, $I_0 = \{0, 1\} \mu\text{A}$, $A = \{1, 2\}$, $R_S = \{0, 0.5\} \Omega$, and $R_P = \{0, 100\} \Omega$. Meanwhile, the TDM has seven unknown parameters to be estimated with the MFO design interval: $I_{PV} = \{0, 1\} \text{ A}$, $I_{01} = \{0, 1\} \mu\text{A}$, $I_{02} = \{0, 1\} \mu\text{A}$, $A_1 = \{1, 2\}$, $A_2 = \{1, 2\}$, $R_S = \{0, 0.5\} \Omega$, and $R_P = \{0, 100\} \Omega$.

Table 1. RTC-France Photovoltaic Cell Data

Item	Measured Data		
	V (Volt)	I (Ampere)	P (Watt)
1	-0.2157	0.7640	-0.1572
2	-0.1291	0.7620	-0.0984
3	-0.0588	0.7605	-0.0447
4	0.0057	0.7605	0.0043
5	0.0646	0.7600	0.0491
6	0.1185	0.7590	0.0899
7	0.1678	0.7570	0.1270
8	0.2132	0.7570	0.1614
9	0.2545	0.7555	0.1923
10	0.2924	0.7540	0.2205
11	0.3269	0.7505	0.2453
12	0.3585	0.7465	0.2676
13	0.3873	0.7385	0.2860
14	0.4137	0.7280	0.3012
15	0.4373	0.7065	0.3090
16	0.4590	0.6755	0.3101
17	0.4784	0.6320	0.3023
18	0.4960	0.5730	0.2842

Item	Measured Data		
	V (Volt)	I (Ampere)	P (Watt)
19	0.5119	0.4990	0.2554
20	0.5265	0.4130	0.2174
21	0.5398	0.3165	0.1708
22	0.5521	0.2120	0.1170
23	0.5633	0.1035	0.0583
24	0.5736	-0.0100	-0.0057
25	0.5833	-0.1230	-0.0717
26	0.5900	-0.2100	-0.1239

Table 2 presents the estimated parameters and the RMSE for ODM and TDM of RTC-France photovoltaic cells using the MFO algorithm.

Table 2. Estimation Results Using the MFO Algorithm

Parameters	ODM	TDM
I_{PV} (A)	0.7608	0.7608
I_{O1} (μ A)	0.3230	0.7493
I_{O2} (μ A)	-	0.2260
R_s (Ω)	0.0364	0.0367
R_p (Ω)	53.7185	55.4854
A_1	1.4812	2.0000
A_2	-	1.4510
RMSE	9.8602×10^{-4}	9.8248×10^{-4}

The RMSE values obtained using the MFO algorithm for the RTC-France photovoltaic cell are presented in Table 2, with 9.8602×10^{-4} for the ODM and 9.8344×10^{-4} for the two-diode model (TDM). These results indicate that the TDM achieves marginally higher accuracy in parameter estimation compared to the ODM, attributed to its enhanced capability to model recombination losses through the inclusion of a second diode. The reduced RMSE of the TDM underscores its suitability for applications requiring precise photovoltaic characterization under varying operational conditions.

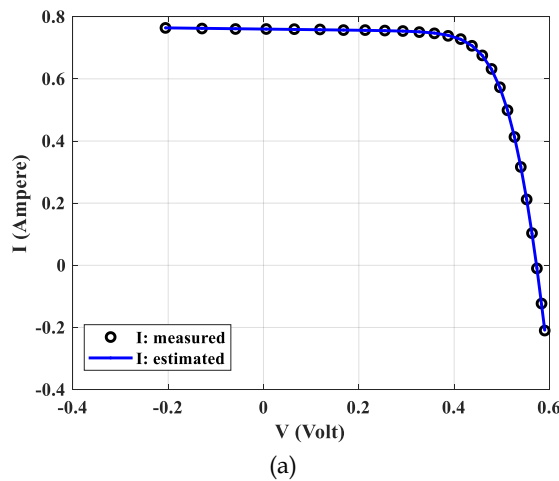
A comparative analysis of photovoltaic parameter estimation methods, as summarized in Table 3, reveals that the MFO algorithm exhibits accuracy comparable to advanced techniques such as teaching-learning-based optimization with triple-phase learning (TPTLBO), improved teaching-learning-based optimization (ITLBO), improved symbiotic organisms search (ISCE), and hybrid firefly and pattern search (HFAPS) for the TDM. For the ODM, the MFO algorithm surpasses the accuracy of symbiotic organisms search (SOS), modified salp swarm optimization (MSSO), and modified artificial bee colony (MABC) algorithms. Furthermore, the MFO algorithm demonstrates superior performance over methods such as supply-demand-based

optimization (SDO), PGJAYA, parallelized sunflower optimization (pSFS), improved crow search algorithm (ImCSA), modified adaptive differential evolution (MADE), chaotic whale optimization algorithm (CWOA), and Nelder-Mead-modified moth-flame optimization (NM-MPSO) in TDM-based parameter estimation. These results validate the MFO algorithm's robustness and precision in navigating complex, high-dimensional search spaces, positioning it as a competitive tool for photovoltaic system optimization.

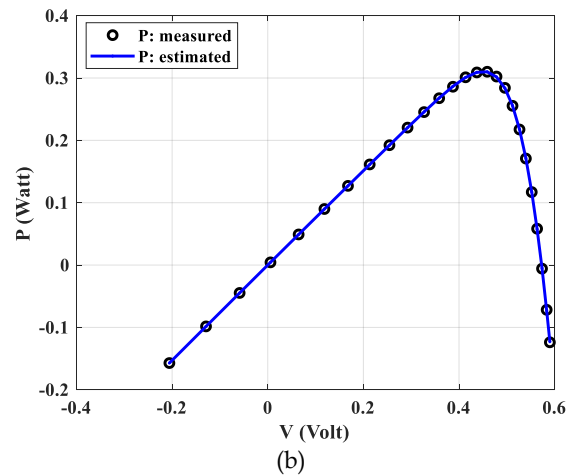
Table 3. Comparison of RMSE Results of RTC-France Photovoltaic Parameter Estimation of Various Algorithms

Algorithms	ODM	TDM
MFO	9.8602×10^{-4}	9.8248×10^{-4}
SDO (Xiong et al., 2019)	9.8602×10^{-4}	9.8250×10^{-4}
SOS (Xiong et al., 2018)	9.8609×10^{-4}	9.8518×10^{-4}
TPTLBO (Liao et al., 2020)	9.8602×10^{-4}	9.8248×10^{-4}
ITLBO (Li et al., 2019)	9.8602×10^{-4}	9.8248×10^{-4}
PGJAYA (Yu et al., 2019)	9.8602×10^{-4}	9.8263×10^{-4}
pSFS (Chen et al., 2019)	9.8602×10^{-4}	9.8255×10^{-4}
ImCSA (Kang et al., 2018)	9.8602×10^{-4}	9.8249×10^{-4}
ISCE (Gao et al., 2018)	9.8602×10^{-4}	9.8248×10^{-4}
MSSO (Lin et al., 2017)	9.8607×10^{-4}	9.8281×10^{-4}
MABC (Jamadi et al., 2016)	9.8610×10^{-4}	9.8276×10^{-4}
MADE (Li et al., 2019)	9.8602×10^{-4}	9.8261×10^{-4}
HFAPS (Beigi & Maroosi, 2018)	9.8602×10^{-4}	9.8248×10^{-4}
CWOA (Oliva et al., 2017)	9.8602×10^{-4}	9.8272×10^{-4}
NM-MPSO (Hamid et al., 2016)	9.8602×10^{-4}	9.8250×10^{-4}

Furthermore, to rigorously validate the accuracy of the MFO algorithm in determining photovoltaic parameters, the current-voltage (I-V) and power-voltage (P-V) curves derived from the measured and estimated datasets were systematically compared. Figures 3(a) and 3(b) illustrate the I-V and P-V characteristics, respectively, for the ODM, while Figures 4(a) and 4(b) depict the corresponding curves for the TDM. A striking congruence between the measured and estimated curves is evident across all figures, with negligible deviations observed in both the I-V and P-V profiles. This close alignment underscores the MFO algorithm's capability to accurately replicate the electrical behavior of photovoltaic systems under both ODM and TDM configurations. The consistent overlap of experimental and simulated curves further substantiates the algorithm's robustness in parameter identification, reinforcing its reliability for high-precision photovoltaic modeling and analysis.



(a)

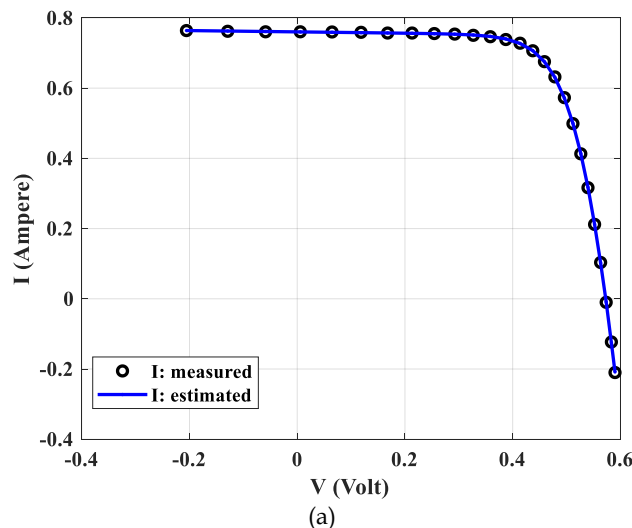


(b)

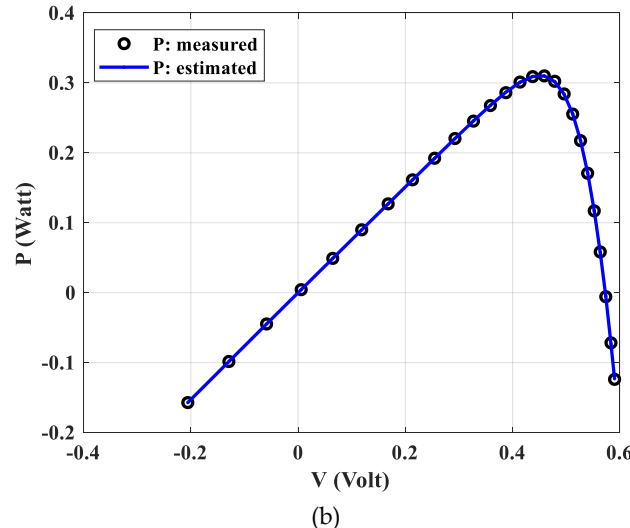
Figure 3. One-diode model: (a) I-V curve, (b) P-V curve

By comparing the measured data with the estimated results, the average current errors for both the ODM and TDM are found to be below 0,0025 A, while the average power errors for these models remain under 0,0015 W. These results demonstrate that the MFO algorithm achieves photovoltaic parameter estimation with exceptional accuracy, as evidenced by the minimal

deviations observed for both the ODM and TDM configurations. The consistently low errors across current and power measurements highlight the robustness of the MFO algorithm in delivering precise parameter identification, reinforcing its suitability for modeling complex photovoltaic systems under varying operational conditions.



(a)



(b)

Figure 4. Two-diode model: (a) I-V curve, (b) P-V curve

Conclusion

The MFO algorithm achieves root mean square error (RMSE) values of 9.8602×10^{-4} and 9.8344×10^{-4} for photovoltaic parameter estimation under the ODM and TDM, respectively. Notably, the marginally lower RMSE of the TDM underscores its superior accuracy over the ODM. Furthermore, comparative analysis demonstrates that the MFO algorithm significantly outperforms existing metaheuristic algorithms including SDO, SOS, MSSO, PGJAYA, psFS, ImCSA, MABC, MADE, CWOA, and NM-MPSO in terms of estimation precision. Beyond

its exceptional accuracy in parameter identification, the MFO algorithm exhibits remarkable fidelity in reconstructing the I-V and P-V curves, aligning closely with empirical measurements. Additionally, the algorithm's robustness and adaptability suggest its broader applicability for optimizing parameters in diverse photovoltaic technologies, including monocrystalline and polycrystalline solar panels, thereby holding significant promise for advancing photovoltaic modeling and system design.

Acknowledgments

The authors would like to express their gratitude to LPPM Universitas Tanjungpura (UNTAN) for the research funding support through DIPA 2024. The authors also extend their appreciation to the Head of LPPM UNTAN for the assistance provided through the same funding scheme.

Author Contributions

Conceptualization, data curation, writing—original draft preparation and methodology, F.H.; validation, formal analysis, writing—review and editing, A.H. All authors have read and agreed to the published version of the manuscript.

Funding

The author declares that this research was funded by DIPA UNTAN in 2024 with assignment agreement letter number: 3711/UN22.4/PT.01.05/2024.

Conflicts of Interest

All authors declare that there is no conflict of interest in and during the writing of this article.

References

Abdel-Basset, M., Mohamed, R., Hezam, I. M., Sallam, K. M., & Hameed, I. A. (2024). Parameters identification of photovoltaic models using Lambert W-function and Newton-Raphson method collaborated with AI-based optimization techniques: A comparative study. *Expert Systems with Applications*, 255(PD), 124777. <https://doi.org/10.1016/j.eswa.2024.124777>

Abdulrazzaq, A. K., Bognár, G., & Plesz, B. (2022). Accurate method for PV solar cells and modules parameters extraction using I-V curves. *Journal of King Saud University - Engineering Sciences*, 34(1). <https://doi.org/10.1016/j.jksues.2020.07.008>

Adak, S., Cangi, H., Yilmaz, A. S., & Arifoglu, U. (2023). Development software program for extraction of photovoltaic cell equivalent circuit model parameters based on the Newton-Raphson method. In *Journal of Computational Electronics* (Vol. 22, Issue 1). <https://doi.org/10.1007/s10825-022-01969-8>

Bakır, H. (2023). Comparative performance analysis of metaheuristic search algorithms in parameter extraction for various solar cell models. *Environmental Challenges*, 11. <https://doi.org/10.1016/j.envc.2023.100720>

Bălăceanu, M., Popa, N. S., Nae, V., Târhoacă, M. C., & Popescu, M. O. (2024). The Influence of Environmental Factors on a Photovoltaic Panel-PVsyst Simulation. *EEA - Electrotehnica, Electronica, Automatica*, 72(2), 03-12. <https://doi.org/10.46904/eea.24.72.2.1108001>

Beigi, A. M., & Maroosi, A. (2018). Parameter identification for solar cells and module using a Hybrid Firefly and Pattern Search Algorithms. *Solar Energy*, 171. <https://doi.org/10.1016/j.solener.2018.06.092>

Čalasan, M., Radonjić, I., Micev, M., Petronijević, M., & Pantić, L. (2024). Voltage root mean square error calculation for solar cell parameter estimation: A novel g-function approach. *Helion*, 10(18). <https://doi.org/10.1016/j.heliyon.2024.e37887>

Çelik, E., Karayel, M., Maden, D., Abdel-salam, M., Öztürk, N., Kaplan, O., Tejani, G. G., Sharma, S. K., & Baljon, M. (2025). Reconfigured single- and double- diode models for improved modelling of solar cells / modules. *Scientific Reports*, 1-19.

Chen, X., Yue, H., & Yu, K. (2019). Perturbed stochastic fractal search for solar PV parameter estimation. *Energy*, 189. <https://doi.org/10.1016/j.energy.2019.116247>

Dkhichi, F. (2023). Parameter extraction of photovoltaic module model by using Levenberg-Marquardt algorithm based on simulated annealing method. *Journal of Computational Electronics*, 22(4). <https://doi.org/10.1007/s10825-023-02058-0>

Durango-Flórez, M., González-Montoya, D., Trejos-Grisales, L. A., & Ramos-Paja, C. A. (2022). PV Array Reconfiguration Based on Genetic Algorithm for Maximum Power Extraction and Energy Impact Analysis. *Sustainability (Switzerland)*, 14(7). <https://doi.org/10.3390/su14073764>

El Ainaoui, K., Zaimi, M., & Assaid, E. M. (2023). Innovative approaches to extract double-diode model physical parameters of a PV module serving outdoors under real-world conditions. *Energy Conversion and Management*, 292. <https://doi.org/10.1016/j.enconman.2023.117365>

Gao, X., Cui, Y., Hu, J., Xu, G., Wang, Z., Qu, J., & Wang, H. (2018). Parameter extraction of solar cell models using improved shuffled complex evolution algorithm. *Energy Conversion and Management*, 157. <https://doi.org/10.1016/j.enconman.2017.12.033>

Hamid, N. F. A., Rahim, N. A., & Selvaraj, J. (2016). Solar cell parameters identification using hybrid Nelder-Mead and modified particle swarm optimization. *Journal of Renewable and Sustainable Energy*, 8(1). <https://doi.org/10.1063/1.4941791>

Jamadi, M., Merrikh-Bayat, F., & Bigdeli, M. (2016). Very accurate parameter estimation of single- and double-diode solar cell models using a modified artificial bee colony algorithm. *International Journal of Energy and Environmental Engineering*, 7(1). <https://doi.org/10.1007/s40095-015-0198-5>

Jannah, N., Gunawan, T. S., Yusoff, S. H., Hanifah, M. S. A., & Sapihie, S. N. M. (2024). Recent Advances and

Future Challenges of Solar Power Generation Forecasting. *IEEE Access*, 12(November), 168904-168924.
<https://doi.org/10.1109/ACCESS.2024.3496120>

Kang, T., Yao, J., Jin, M., Yang, S., & Duong, T. (2018). A novel improved cuckoo search algorithm for parameter estimation of photovoltaic (PV) models. *Energies*, 11(5).
<https://doi.org/10.3390/en11051060>

Kwakye, B. D., Li, Y., Mohamed, H. H., Baidoo, E., & Asenso, T. Q. (2024). Particle guided metaheuristic algorithm for global optimization and feature selection problems[Formula presented]. *Expert Systems with Applications*, 248.
<https://doi.org/10.1016/j.eswa.2024.123362>

Li, S., Gong, W., Yan, X., Hu, C., Bai, D., & Wang, L. (2019). Parameter estimation of photovoltaic models with memetic adaptive differential evolution. *Solar Energy*, 190.
<https://doi.org/10.1016/j.solener.2019.08.022>

Li, S., Gong, W., Yan, X., Hu, C., Bai, D., Wang, L., & Gao, L. (2019). Parameter extraction of photovoltaic models using an improved teaching-learning-based optimization. *Energy Conversion and Management*, 186.
<https://doi.org/10.1016/j.enconman.2019.02.048>

Liao, Z., Chen, Z., & Li, S. (2020). Parameters Extraction of Photovoltaic Models Using Triple-Phase Teaching-Learning-Based Optimization. *IEEE Access*, 8.
<https://doi.org/10.1109/ACCESS.2020.2984728>

Lin, H., Wang, G., Su, Q., Han, C., Xue, C., Yin, S., Fang, L., Xu, X., & Gao, P. (2024). Unveiling the mechanism of attaining high fill factor in silicon solar cells. *Progress in Photovoltaics: Research and Applications*, 32(6).
<https://doi.org/10.1002/pip.3775>

Lin, P., Cheng, S., Yeh, W., Chen, Z., & Wu, L. (2017). Parameters extraction of solar cell models using a modified simplified swarm optimization algorithm. *Solar Energy*, 144.
<https://doi.org/10.1016/j.solener.2017.01.064>

Lo, W. L., Chung, H. S. H., Hsung, R. T. C., Fu, H., & Shen, T. W. (2024). PV Panel Model Parameter Estimation by Using Particle Swarm Optimization and Artificial Neural Network. *Sensors*, 24(10).
<https://doi.org/10.3390/s24103006>

Morcillo, J., Castaneda, M., Jimenez, M., Zapata, S., Dyner, I., & Aristizabal, A. J. (2022). Assessing the speed, extent, and impact of the diffusion of solar PV. *Energy Reports*, 8.
<https://doi.org/10.1016/j.egyr.2022.06.099>

Nfaoui, M., Ihfa, F. E., Bougtaib, A., Harfouf, A. El, Hayani-Mounir, S., Bennai, M., & El-Hami, K. (2024). Comprehensive modeling and simulation of photovoltaic system performance by using matlab/simulink: integrating dynamic meteorological parameters for enhanced accuracy. *Journal of Umm Al-Qura University for Applied Sciences*, 0123456789.
<https://doi.org/10.1007/s43994-024-00175-5>

Oliva, D., Abd El Aziz, M., & Ella Hassanien, A. (2017). Parameter estimation of photovoltaic cells using an improved chaotic whale optimization algorithm. *Applied Energy*, 200.
<https://doi.org/10.1016/j.apenergy.2017.05.029>

Pindado, S., Roibas-Millan, E., Cubas, J., Alvarez, J. M., Alfonso-Corcuera, D., Cubero-Estalrich, J. L., Gonzalez-Estrada, A., Sanabria-Pinzon, M., & Jado-Puente, R. (2021). Simplified Lambert W-Function Math Equations When Applied to Photovoltaic Systems Modeling. *IEEE Transactions on Industry Applications*, 57(2).
<https://doi.org/10.1109/TIA.2021.3052858>

Saadaoui, D., Elyaqouti, M., Assalaou, K., Ben hmamou, D., & Lidaighbi, S. (2021). Parameters optimization of solar PV cell/module using genetic algorithm based on non-uniform mutation. In *Energy Conversion and Management: X* (Vol. 12).
<https://doi.org/10.1016/j.ecmx.2021.100129>

Sakthivel, S. S., Gokulakrishnan, L., Arunachaleashwer, S., Lokesh, V., & Venkadesan, A. (2023). Parameter Estimation of a Single Diode Model of a PV Panel using Gauss-Seidel Method: An Experimental Validation. *2023 International Conference for Advancement in Technology, ICONAT 2023*.
<https://doi.org/10.1109/ICONAT57137.2023.10080499>

Tifidat, K., Maouhoub, N., Askar, S. S., & Abouhawwash, M. (2023). Numerical procedure for accurate simulation of photovoltaic modules performance based on the identification of the single-diode model parameters. *Energy Reports*, 9.
<https://doi.org/10.1016/j.egyr.2023.04.378>

Tifidat, K., Maouhoub, N., Benahmida, A., & Ezzahra Ait Salah, F. (2022). An accurate approach for modeling I-V characteristics of photovoltaic generators based on the two-diode model. *Energy Conversion and Management*: X, 14.
<https://doi.org/10.1016/j.ecmx.2022.100205>

Wang, J., Wei, H., Dou, S., Gillbanks, J., & Zhao, X. (2024). Active Disturbance Rejection Control Based on an Improved Topology Strategy and Padé Approximation in LCL-Filtered Photovoltaic Grid-Connected Inverters. *Applied Sciences (Switzerland)*, 14(23).
<https://doi.org/10.3390/app142311133>

Xiong, G., Zhang, J., Shi, D., & Yuan, X. (2019). Application of Supply-Demand-Based

Optimization for Parameter Extraction of Solar Photovoltaic Models. *Complexity*, 2019. <https://doi.org/10.1155/2019/3923691>

Xiong, G., Zhang, J., Yuan, X., Shi, D., & He, Y. (2018). Application of symbiotic organisms search algorithm for parameter extraction of solar cell models. *Applied Sciences (Switzerland)*, 8(11). <https://doi.org/10.3390/app8112155>

Yu, K., Qu, B., Yue, C., Ge, S., Chen, X., & Liang, J. (2019). A performance-guided JAYA algorithm for parameters identification of photovoltaic cell and module. *Applied Energy*, 237. <https://doi.org/10.1016/j.apenergy.2019.01.008>

Yuan, S., Ji, Y., Chen, Y., Liu, X., & Zhang, W. (2023). An Improved Differential Evolution for Parameter Identification of Photovoltaic Models. *Sustainability (Switzerland)*, 15(18). <https://doi.org/10.3390/su151813916>